ACS OMEGA

http://pubs.acs.org/journal/acsodf

Article

Identifying Lipid Metabolites Influenced by Oleic Acid Administration Using High-Performance Liquid Chromatography–Mass Spectrometry-Based Lipidomics

Chao Xu, Dan Song, Askild L. Holck, Youyou Zhou, and Rong Liu*

Cite This: *ACS Omega* 2020, 5, 11314–11323

Read Online

ACCESS | Metrics & More | Article Recommendations

ABSTRACT: Oleic acid (OA), one of the most important monounsaturated fatty acids, possesses protective properties against chronic liver disease (CLD) development, but the underlying metabolic metabolism remains unknown. HPLC−MS-based lipidomics was utilized to identify and quantify the endogenously altered lipid metabolites when hepatocytes were exposed to OA administration. The identified lipids could be grouped into 22 lipid classes; of which, 10 classes were significantly influenced by the OA treatment: lysophosphatidylcholine (LPC), phosphatidylglycerol (PG), ceramides (Cer), hexosylceramides (Hex1Cer), dihexosylceramides (Hex2Cer), cholesterol ester (ChE), and coenzyme (Co) were decreased, while diglyceride (DG), triglyceride (TG), and acyl carnitine (AcCa) were increased. In addition, as the variable importance in projection (VIP) list (VIP > 1.0 and $P < 0.05$) showed, 478 lipid species showed significant difference with OA administration, and these molecules could be potential biomarkers in conjunction with OA administration. In summary, our results provided a novel perspective to understand the influences of OA administration by investigating endogenous altered levels of lipid metabolites via lipidomics.

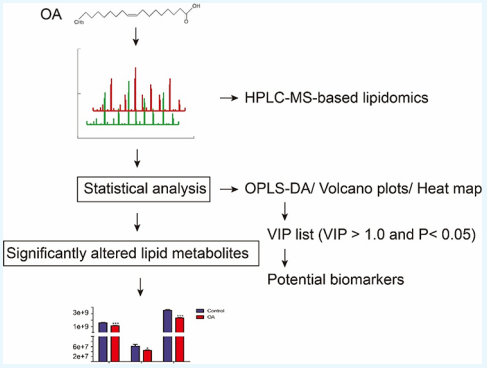

INTRODUCTION

Fatty acids (FA), as one of the most important components of lipids, are associated with growth, development, and disease.[1] According to the number of double bonds, FA can be divided into three types, saturated fatty acids (SFAs), monounsaturated fatty acids (MUFAs), and polyunsaturated fatty acids (PUFAs). All of them are linked to human health. Among them, enriched-monounsaturated fatty acid diets have positive effects on chronic liver disease (CLD) prevention.[2] Being the predominant monounsaturated fatty acid, oleic acid (OA) has attracted increasing attention in CLD treatment.

CLD is one of the most common public health problems, and, at the early stage, it is usually linked to the liver fibrosis. Liver fibrosis may worsen into cirrhosis and finally to hepatocellular carcinoma (HCC).[3] Meanwhile, non-alcoholic fatty liver disease (NAFLD) and non-alcoholic steatohepatitis (NASH) could progress to CLD via liver fibrosis.[3] Various underlying mechanisms of liver disease progression have been demonstrated, and, among them, endoplasmic reticulum (ER) stress and lipotoxicity are generally involved in the progression of liver disease.[4,5] In fact, SFAs, especially palmitic acid (PA), are toxic for the liver by inducing ER stress and lipotoxicity.[6,7] However, OA is able to suppress the deleterious effects induced by SFAs.

Evidence has shown that OA could suppress PA-induced negative effects on ER stress and lipoapoptosis in hepatocytes via inhibiting the activation of ribosomal protein S6 kinase 1 (S6K1) and, as a consequence, attenuate the progression of NAFLD.[8] Similarly, OA could attenuate the PA-induced hepatic lipotoxicity in both hepatocytes and a NASH model through preventing hepatocytic apoptosis, which is a critical pathogenic feature of NASH. OA is involved in regulating lipid metabolism. The protective effects alleviate the pathological development from steatosis to NASH.[9] Besides, OA could ameliorate hepatic steatosis and fibrosis in an NAFLD animal model by increasing the excretion of hepatic triglycerides and decreasing the levels of several inflammatory molecules, thus attenuating every step of NAFLD progression.[10]

Actually, CLD is characterized as the hepatic manifestation of the metabolic syndrome and is closely associated with disordered lipid metabolism, while OA could regulate lipogenesis and lipid secretion in HepG2 cells.[11,12] However,

Received: December 21, 2019
Accepted: April 14, 2020
Published: April 29, 2020

https://dx.doi.org/10.1021/acsomega.9b04402
ACS Omega 2020, 5, 11314–11323

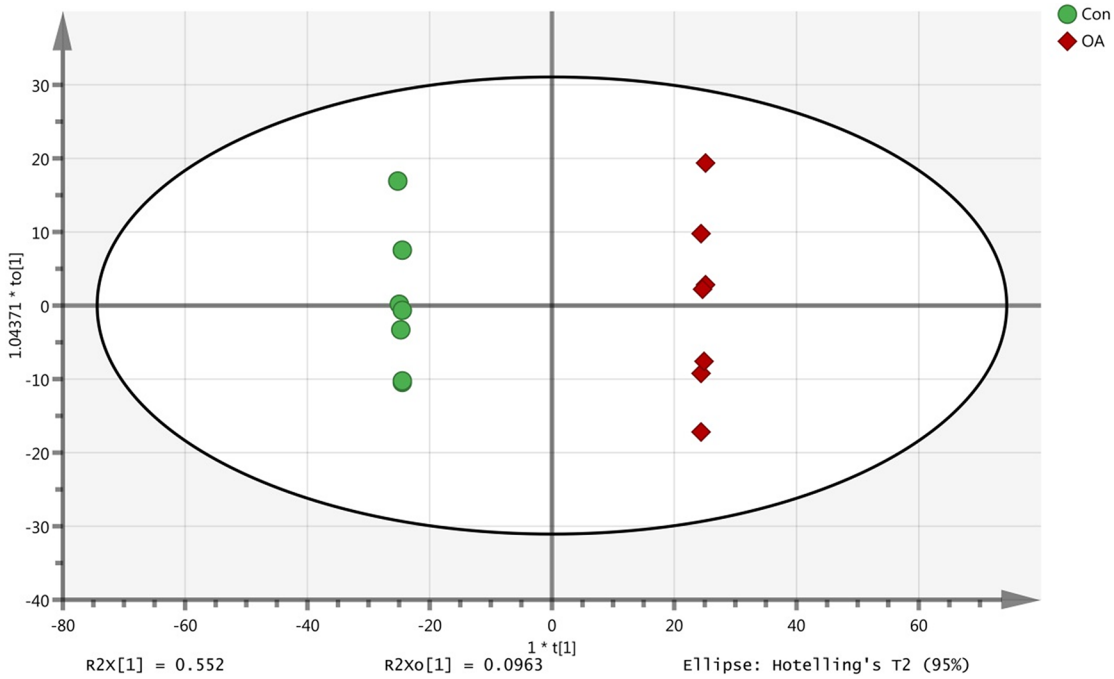

Figure 1. OPLS-DA score plots of OA-treated groups (n = 7, red diamonds) and control groups (n = 7, green circles).

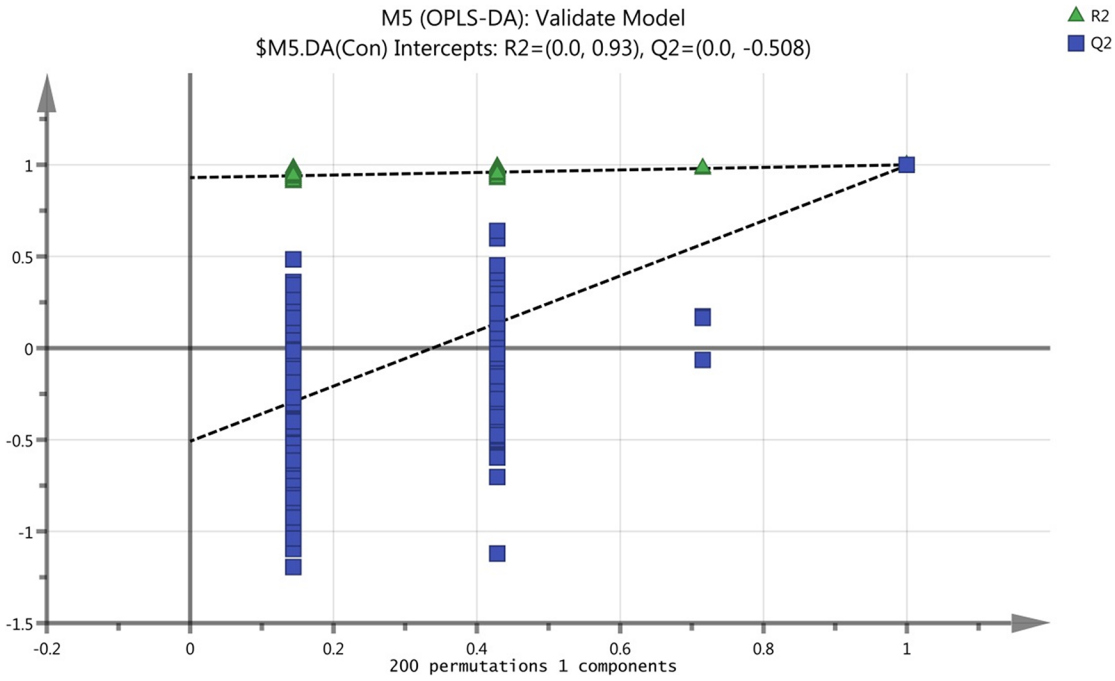

Figure 2. Validation plots of responses to 200 permutations of the OPLS-DA model. The R^2 and Q^2 were 0.93 and 0.607, respectively.

the underlying metabolic metabolism of OA remains unclear. Consequently, we utilize lipidomics which relies on the development and application of mass spectrometry (MS) to identify and quantify the endogenous changes in lipid concentrations after OA treatment.[13,14] Lipidomics, as a significant branch of metabolomics, has been dramatically developing since it was presented in 2003. It provided a new perspective to intuitively visualize the changes of lipid metabolites when exposed to physiological changes and stimulation conditions.[14]

In summary, in this study, HPLC−MS-based lipidomics was utilized to investigate endogenous changes in lipid metabolite concentrations with OA administration, and this technique provided a novel insight revealing the effects of OA administration on lipid metabolism in hepatocytes.

RESULTS

Statistical Analysis of Lipid Metabolites from OA-Treated Groups and Control Groups. Principal component analysis (PCA)[15] and orthogonal partial least squares discriminant analysis (OPLS-DA)[16] score plots were per-

https://dx.doi.org/10.1021/acsomega.9b04402
ACS Omega 2020, 5, 11314−11323

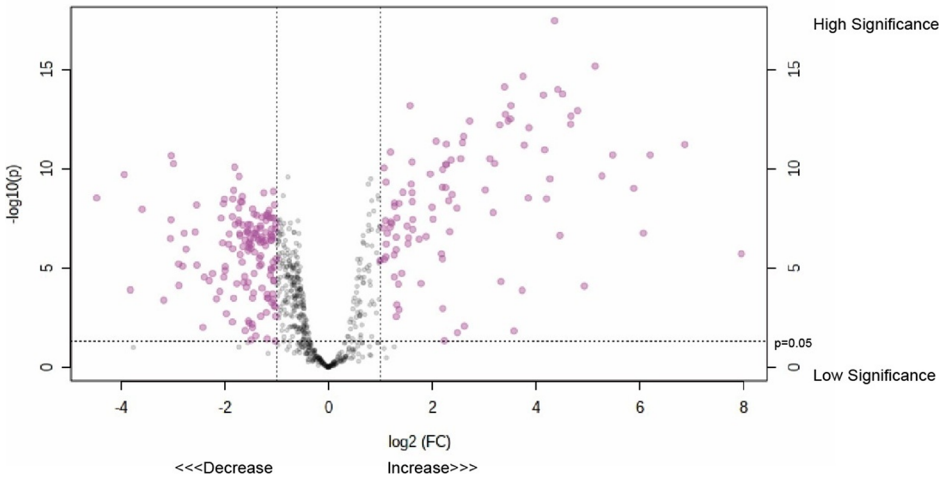

Figure 3. Volcano plots were obtained from all of identified molecules from the positive and negative modes. The threshold change was set as 2.0. The red points are the metabolites presented at significantly different amounts after OA treatment. Black points indicate compounds not influenced by OA treatment. The lipid metabolites to the right of the right threshold increase with OA administration, while those to the left of the left threshold decrease. FC = fold change.

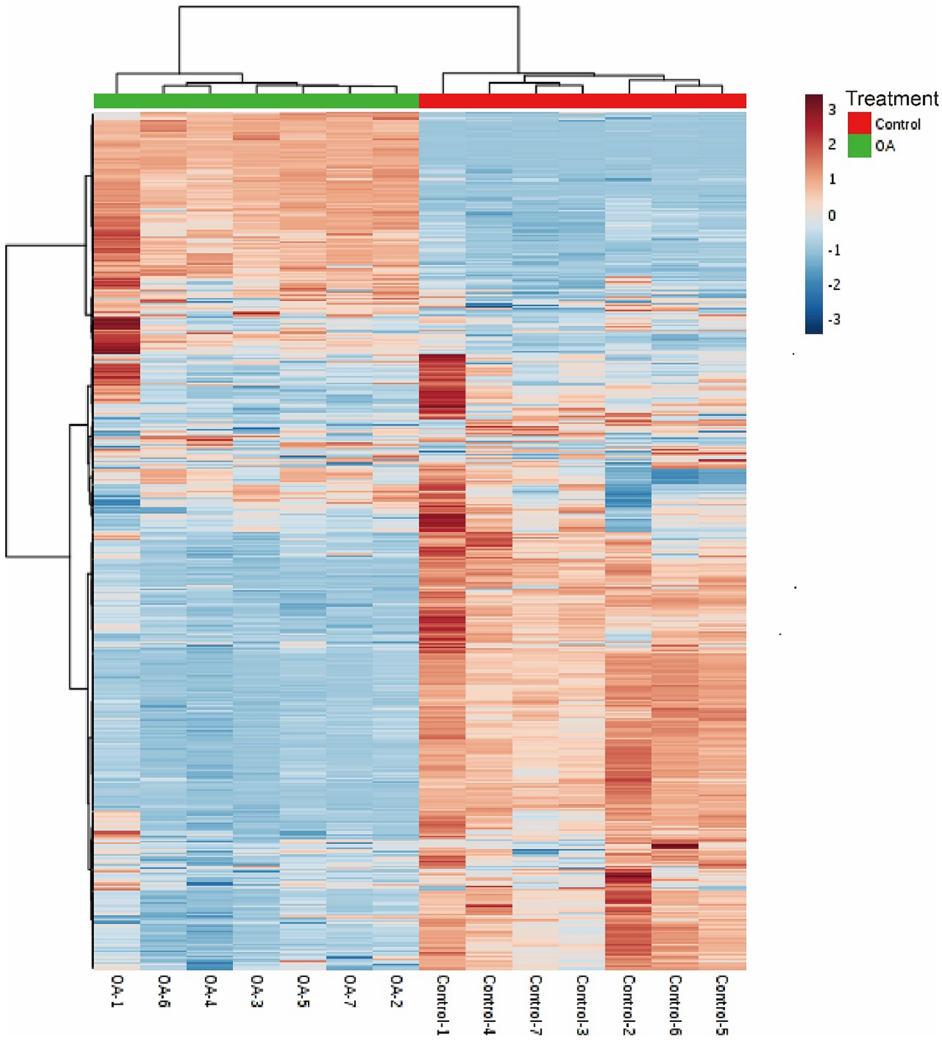

Figure 4. Heat map of endogenous metabolites between OA-treated groups (n = 7) and control groups (n = 7). The heat map was obtained from all identified lipids from the positive and negative modes. Red-filled and blue-filled lines indicate increased and decreased levels of lipids, respectively. The fold change is indicated.

https://dx.doi.org/10.1021/acsomega.9b04402
ACS Omega 2020, 5, 11314−11323

formed to determine the differences between OA-treated groups and control groups (Figure 1). Obviously, a distinct separation between OA-treated groups and control groups was observed in the PCA score plots, and the same trend was detected in OPLS-DA score plots. A high repeatability of each group was also detected. In addition, 200 times of chance permutations[17] were carried out to evaluate the predictability of the OPLS-DA model (Figure 2). The R^2 and Q^2 values were 0.93 and 0.607, respectively, and the y intercept was −0.508. The R^2 reflected the difference of the principal components, and the closer R^2 gets to 1, the more different the principal component gets. Q^2 represented the predictability of the OPLS-DA model. Only when $Q^2 > 0.5$, the OPLS-DA model possessed predictability. The negative y intercept indicated that the model was not overfitting.[17] Taken together, OPLS-DA analysis presented significant separation and positive predictability.

More than 1000 different lipid compounds were identified in the OA-treated and control groups. Volcano plots based on all of the identified lipid metabolites are presented in Figure 3. As reported, the parameters of significance threshold and fold change set at $P < 0.05$ and 1.2, respectively, were enough to identify metabolites with significant difference.[16] In our results, a large number of lipids were present at significantly higher or lower amounts for the fold change set at 2.0, which was more valid, indicating that OA administration significantly regulated lipid metabolism.

The heat map[18] obtained from all of the identified lipid metabolites was used to directly visualize the trend of lipid metabolite changes after OA treatment and assess their hierarchical cluster. As the heat map result showed, a large proportion of lipid metabolites was decreased after OA treatment (Figure 4).

The variable importance in projection (VIP) list (VIP > 1.0 and $P < 0.05$)[16] was obtained from OPLS-DA, showing the components most influenced by the OA treatment.

Identification of Lipid Metabolites by HPLC−MS. The identified lipids influenced by OA treatment were grouped into 22 classes belonging to the four categories including phospholipids, sphingolipids, neutral lipids, and "fatty acyl and other lipids". The 22 classes were as follows: phospholipids: lysophosphatidylethanolamine (LPE), lysophosphatidylcholine (LPC), phosphatidylglycerol (PG), phosphatidylinositol (PI), phosphatidylserine (PS), phosphatidylethanolamine (PE), phosphatidylcholine (PC), and cardiolipin (CL); sphingolipids: hexosylceramides (Hex1Cer), trihexosylceramides (Hex3Cer), ceramides (Cer), sphingomyelin (SM), gangliosides (GM3), sphingosine (SPH), and dihexosylceramides (Hex2Cer); neutral lipids: cholesterol ester (ChE), diglyceride (DG), and triglyceride (TG); and fatty acyl and other lipids: *N*-acylethanolamine (AEA), FA, acyl carnitine (AcCa), and coenzyme (Co). The summary signals for the identified lipid classes between OA-treated groups and control groups are presented in Table 1.

Significant Changes of Lipid Metabolites in OA-Treated Groups. The statistical results obtained from Table 1 followed by t-tests were used for comparing differences in the summary signals for the compounds in each of the 22 identified lipid classes between OA-treated groups and control groups. Differences were detected in 10 of the 22 classes (Figure 5). First, LPC and PG were significantly decreased when comparing with control groups. Second, Hex1Cer, Hex2Cer, and Cer presented similar trends, and they were dramatically reduced after OA treatment. As components of neutral lipids, ChE was notably decreased, conversely, DG and TG were both increased when comparing with control groups, and TG presented significant difference, while the change in absolute of DG was relatively small. Furthermore, AcCa and Co as constituents of fatty acyl compounds showed an opposite tendency. The content of AcCa was clearly elevated by OA treatment, while Co was significantly decreased in OA-treated groups.

Additionally, changes in LPC (18:0) and PG (16:0_18:1) (Figure 6), Cer (d18:1_22:0) and Cer (d18:1_24:0) (Figure 7), Hex1Cer (d18:1_22:0), Hex1Cer (d18:1_23:0), Hex1Cer (d18:1_24:0), and Hex1Cer (d18:1_24:1) (Figure 8), and ChE (22,6) (Figure 9) were shown as representative lipids involved in liver disease development. These were all significantly decreased with OA administration.

DISCUSSION

In this study, lipidomics based on HPLC−MS was used to identify and quantify lipid compounds. As the results showed, more than 1000 lipid species were identified and grouped into four lipid categories, containing phospholipids, sphingolipids, neutral lipids, and "fatty acyl and other lipids". Among them, some lipid classes were significantly influenced by OA treatment.

Phospholipids remained generally relatively constant with OA administration, except for LPC and PG, which were significantly decreased after OA treatment. LPC was regarded as the death effector of lipoapoptosis in hepatocytes, stimulating the development of NAFLD, and, as a consequence, the content of LPC in the liver of patients with NAFLD was significantly higher than that of control groups. Also, the content of LPC in the liver of patients with NASH seemed to be higher than in NAFLD groups.[19] Furthermore, LPC (18:0) is considered as a biomarker of NAFLD progression and was detected by LC-MS-based lipidomics.[20] Berberine showed therapeutic effects on NAFLD via modulating the lipid metabolism. Particularly, LPC (18:0) was significantly decreased after berberine treatment.[21] Similarly, as the VIP list showed, LPC (18:0) was significantly decreased after OA treatment. Therefore, the decreased levels of LPC after OA treatment may potentially excellently explain the effect of OA administration on CLD treatment. The content of PG was dramatically increased in the mice model of NAFLD, and PG (16:0_18:1) was regarded as the potential biomarker of NAFLD.[22] Conversely, PG (16:0_18:1) was significantly decreased with OA administration. Hence, the attenuation of PG would be one of the potential lipid targets of OA administration on NAFLD prevention, and PG (16:0_18:1) could be a potential biomarker of OA on NAFLD prevention.

Sphingolipid changes were detected after OA treatment, and different tendencies were presented among the classes of sphingolipids, but Cer, Hex1Cer, and Hex2Cer were all significantly reduced comparing with control groups. As reported, the content of Cer was significantly elevated in the diet-induced NAFLD mice model. Myriocin-induced inhibition of Cer synthesis did rescue the hepatocyte disarray and reduced lipid accumulation, inflammation, and fibrosis, indicating that inhibited Cer synthesis would attenuate NAFLD development.[23] Similar results were observed in mice with NAFLD where myriocin inhibited ceramide *de novo* synthesis and subsequently reduced hepatotoxic lipid accumu-

https://dx.doi.org/10.1021/acsomega.9b04402
ACS Omega 2020, 5, 11314−11323

Table 1. Summary Signals for the Identified Lipid Classes between OA-Treated Groups and Control Groups

lipid species	Con-7	Con-6	Con-5	Con-4	Con-3	Con-2	Con-1	OA-7	OA-6	OA-5	OA-4	OA-3	OA-2	OA-1
LPE	5.42×10^{7}	6.19×10^{7}	6.64×10^{7}	4.60×10^{7}	2.02×10^{7}	2.29×10^{7}	1.11×10^{8}	2.68×10^{7}	1.93×10^{7}	5.01×10^{7}	5.18×10^{7}	1.97×10^{7}	2.01×10^{7}	1.76×10^{7}
LPC	1.22×10^{9}	1.49×10^{9}	1.47×10^{9}	1.40×10^{9}	1.19×10^{9}	8.66×10^{8}	1.79×10^{9}	7.71×10^{8}	6.98×10^{8}	7.95×10^{8}	6.35×10^{8}	8.81×10^{8}	9.59×10^{8}	5.00×10^{8}
PG	2.73×10^{9}	3.20×10^{9}	3.08×10^{9}	2.80×10^{9}	2.68×10^{9}	3.33×10^{9}	3.18×10^{9}	2.65×10^{9}	2.30×10^{9}	2.53×10^{9}	2.24×10^{9}	2.54×10^{9}	2.72×10^{9}	2.66×10^{9}
PI	7.02×10^{9}	6.67×10^{9}	6.76×10^{9}	7.64×10^{9}	6.98×10^{9}	7.63×10^{9}	8.34×10^{9}	7.24×10^{9}	6.74×10^{9}	7.41×10^{9}	6.45×10^{9}	6.76×10^{9}	7.30×10^{9}	7.21×10^{9}
PS	7.64×10^{9}	7.70×10^{9}	7.83×10^{9}	8.47×10^{9}	8.94×10^{9}	1.07×10^{10}	9.19×10^{9}	9.74×10^{9}	8.80×10^{9}	9.52×10^{9}	8.74×10^{9}	9.34×10^{9}	9.12×10^{9}	1.07×10^{10}
PE	5.66×10^{10}	6.55×10^{10}	6.30×10^{10}	6.04×10^{10}	5.66×10^{10}	6.94×10^{10}	6.34×10^{10}	6.03×10^{10}	5.64×10^{10}	6.13×10^{10}	5.52×10^{10}	5.90×10^{10}	6.19×10^{10}	6.48×10^{10}
PC	2.78×10^{11}	3.34×10^{11}	3.18×10^{11}	2.89×10^{11}	2.77×10^{11}	3.47×10^{11}	3.23×10^{11}	2.87×10^{11}	2.66×10^{11}	2.91×10^{11}	2.63×10^{11}	2.80×10^{11}	3.01×10^{11}	3.13×10^{11}
CL	6.90×10^{9}	8.05×10^{9}	7.79×10^{9}	8.31×10^{9}	7.58×10^{9}	7.53×10^{9}	9.52×10^{9}	7.88×10^{9}	7.27×10^{9}	7.01×10^{9}	6.67×10^{9}	6.55×10^{9}	7.66×10^{9}	9.51×10^{9}
Hex1-Cer	1.32×10^{9}	1.69×10^{9}	1.61×10^{9}	1.52×10^{9}	1.37×10^{9}	1.88×10^{9}	1.65×10^{9}	1.12×10^{9}	1.07×10^{9}	1.22×10^{9}	9.29×10^{8}	1.08×10^{9}	1.23×10^{9}	1.31×10^{9}
Hex3-Cer	2.39×10^{9}	2.59×10^{9}	2.57×10^{9}	2.70×10^{9}	2.38×10^{9}	2.96×10^{9}	2.90×10^{9}	2.66×10^{9}	2.43×10^{9}	2.78×10^{9}	2.27×10^{9}	2.52×10^{9}	2.83×10^{9}	3.01×10^{9}
Cer	3.14×10^{9}	3.80×10^{9}	3.50×10^{9}	3.38×10^{9}	3.22×10^{9}	3.79×10^{9}	3.85×10^{9}	2.37×10^{9}	2.06×10^{9}	2.55×10^{9}	2.08×10^{9}	2.25×10^{9}	2.53×10^{9}	2.46×10^{9}
SM	1.31×10^{11}	1.60×10^{11}	1.50×10^{11}	1.37×10^{11}	1.30×10^{11}	1.65×10^{11}	1.59×10^{11}	1.46×10^{11}	1.31×10^{11}	1.47×10^{11}	1.23×10^{11}	1.41×10^{11}	1.56×10^{11}	1.59×10^{11}
GM3	4.34×10^{8}	9.93×10^{7}	1.44×10^{8}	5.06×10^{8}	3.73×10^{8}	1.89×10^{8}	5.48×10^{8}	5.09×10^{8}	5.44×10^{8}	5.64×10^{8}	4.50×10^{8}	3.29×10^{8}	3.54×10^{8}	3.85×10^{8}
SPH	3.09×10^{7}	3.92×10^{7}	3.50×10^{7}	3.66×10^{7}	3.39×10^{7}	3.73×10^{7}	3.62×10^{7}	4.28×10^{7}	3.72×10^{7}	3.98×10^{7}	3.49×10^{7}	3.93×10^{7}	5.03×10^{7}	3.53×10^{7}
Hex2-Cer	5.96×10^{7}	5.19×10^{7}	4.90×10^{7}	7.35×10^{7}	7.68×10^{7}	3.08×10^{7}	8.86×10^{7}	4.14×10^{7}	3.49×10^{7}	4.71×10^{7}	4.60×10^{7}	5.35×10^{7}	4.90×10^{7}	3.79×10^{7}
ChE	1.88×10^{7}	2.25×10^{7}	2.30×10^{7}	2.07×10^{7}	1.77×10^{7}	2.37×10^{7}	2.04×10^{7}	2.29×10^{6}	2.83×10^{6}	2.97×10^{6}	2.79×10^{6}	2.29×10^{6}	2.51×10^{6}	2.89×10^{6}
DG	8.38×10^{8}	1.04×10^{9}	9.52×10^{8}	9.59×10^{8}	8.06×10^{8}	6.83×10^{8}	1.23×10^{9}	1.48×10^{9}	1.36×10^{9}	1.60×10^{9}	1.22×10^{9}	1.30×10^{9}	1.52×10^{9}	9.71×10^{8}
TG	2.82×10^{9}	3.17×10^{9}	2.77×10^{9}	2.73×10^{9}	2.64×10^{9}	3.16×10^{9}	2.91×10^{9}	1.90×10^{10}	2.02×10^{10}	1.91×10^{10}	1.83×10^{10}	2.00×10^{10}	1.91×10^{10}	1.90×10^{10}
AEA	1.09×10^{7}	1.37×10^{7}	1.23×10^{7}	1.10×10^{7}	1.17×10^{7}	1.25×10^{7}	1.34×10^{7}	1.23×10^{7}	1.19×10^{7}	1.43×10^{7}	1.11×10^{7}	1.16×10^{7}	1.23×10^{7}	1.07×10^{7}
FA	3.41×10^{10}	3.52×10^{10}	4.04×10^{10}	3.24×10^{10}	3.61×10^{10}	2.97×10^{10}	5.13×10^{10}	2.93×10^{10}	3.88×10^{10}	3.56×10^{10}	3.98×10^{10}	3.79×10^{10}	2.06×10^{10}	3.40×10^{10}
AcCa	1.70×10^{8}	2.43×10^{8}	2.36×10^{8}	7.87×10^{7}	7.05×10^{7}	1.95×10^{8}	1.25×10^{8}	5.72×10^{8}	5.90×10^{8}	6.95×10^{8}	3.13×10^{8}	3.37×10^{8}	3.95×10^{8}	9.85×10^{8}
Co	8.21×10^{8}	9.13×10^{8}	9.08×10^{8}	8.03×10^{8}	8.16×10^{8}	1.14×10^{9}	8.53×10^{8}	7.21×10^{8}	7.02×10^{8}	7.20×10^{8}	6.25×10^{8}	5.69×10^{8}	6.77×10^{8}	8.70×10^{8}

https://dx.doi.org/10.1021/acsomega.9b04402
ACS Omega 2020, 5, 11314−11323

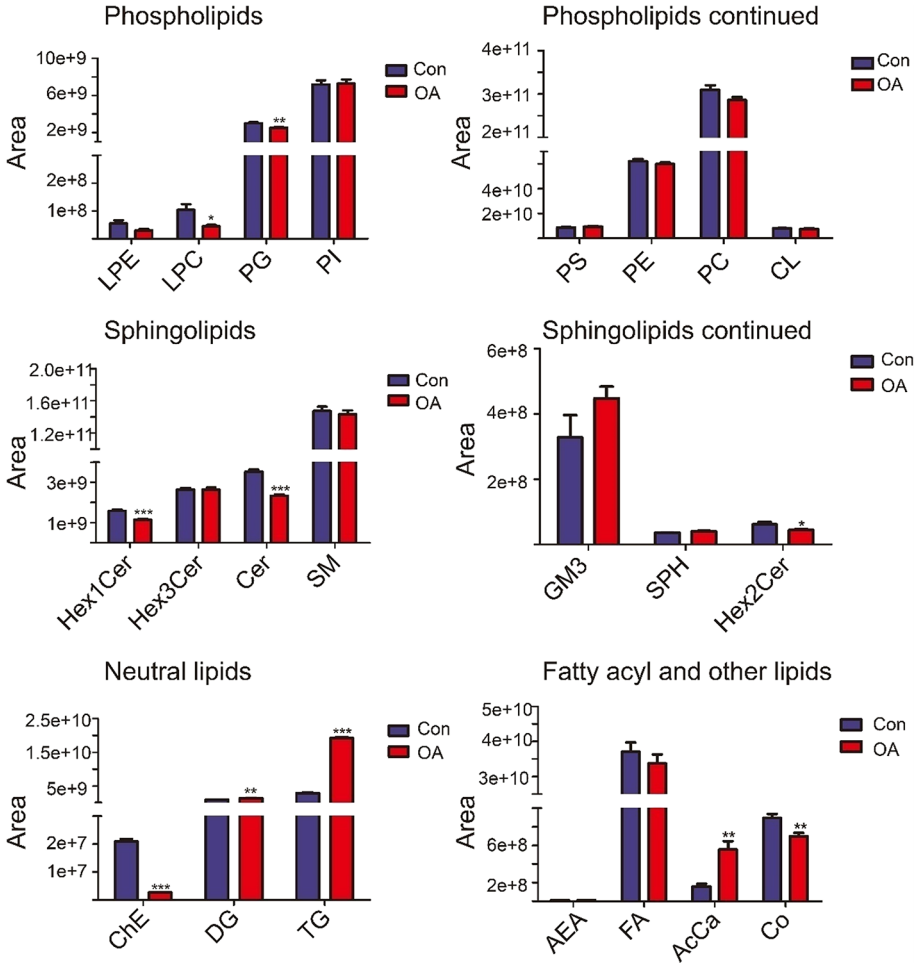

Figure 5. Statistical histogram of 22 lipid classes detected after OA treatment. The blue histograms are control groups, and the red histograms are OA-treated groups. T-tests were carried out subsequently. $P < 0.05$ was considered statistically significant. *$P < 0.05$, **$P < 0.01$, ***$P < 0.001$ vs the controls. LPE: lysophosphatidylethanolamine, LPC: lysophosphatidylcholine, PG: phosphatidylglycerol, PI: phosphatidylinositol, PS: phosphatidylserine, PE: phosphatidylethanolamine, PC: phosphatidylcholine, and CL: cardiolipin; Hex1Cer: hexosylceramides, Hex3Cer: trihexosylceramides, Cer: ceramides, SM: sphingomyelin, GM3: gangliosides, SPH: sphingosine, Hex2Cer: dihexosylceramides; ChE: cholesterol ester, DG: diglyceride, and TG: triglyceride; and fatty acyl and other lipids: AEA: *N*-acylethanolamine, FA: fatty acids, AcCa: acyl carnitine, and Co: coenzyme.

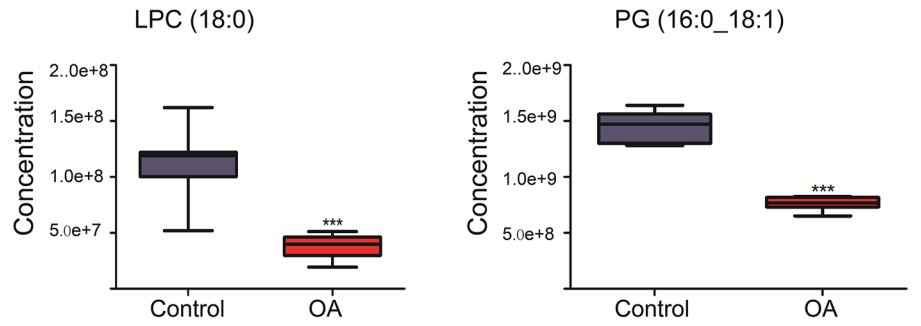

Figure 6. Boxplots of representative lysophosphatidylcholine (LPC) and phosphatidylglycerol (PG) species found significantly decreased in OA-treated groups comparing with control groups. The blue histograms are control groups, and the red histograms are OA-treated groups. T-tests were carried out subsequently. $P < 0.05$ was considered statistically significant. *$P < 0.05$, **$P < 0.01$, ***$P < 0.001$ vs the control.

lation; hence, the inhibition of Cer synthesis was considered as a novel target for NAFLD prevention.[24] Furthermore, the concentration of total and some certain Cer was assessed in the patients with NAFLD, and the results showed that the level of total Cer was significantly increased and Cer (d18:1_16:0), Cer (d18:1_18:0), Cer (d18:1_22:0), and Cer (d18:1_24:0) were markedly higher than in the reference group.[25] The total content of Cer was decreased with OA administration, and Cer (d18:1_22:0) and Cer (d18:1_24:0) were significantly decreased after OA treatment. Hence, OA may exhibit a protective effect on NAFLD development via decreasing the concentration of Cer. Thus, Cer (d18:1_22:0). Besides, accumulated Hex1Cer was positively associated with the risk of liver diseases, such as chronic hepatitis C (CHC), NASH,

https://dx.doi.org/10.1021/acsomega.9b04402
ACS Omega 2020, 5, 11314−11323

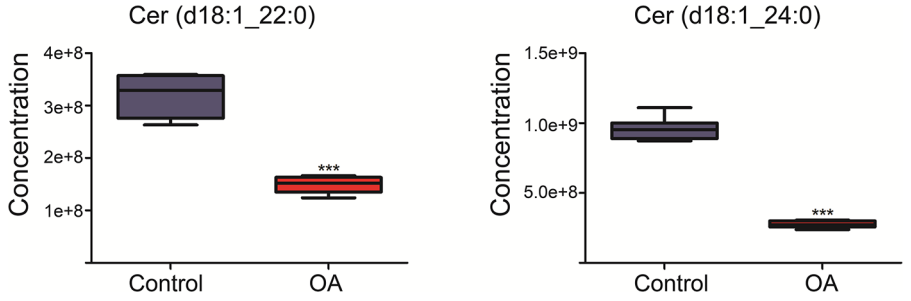

Figure 7. Boxplots of representative ceramides (Cer) species found significantly decreased in OA-treated groups comparing with control groups. The blue histograms are control groups, and the red histograms are OA-treated groups. T-tests were carried out subsequently. $P < 0.05$ was considered statistically significant. *$P < 0.05$, **$P < 0.01$, ***$P < 0.001$ vs the control.

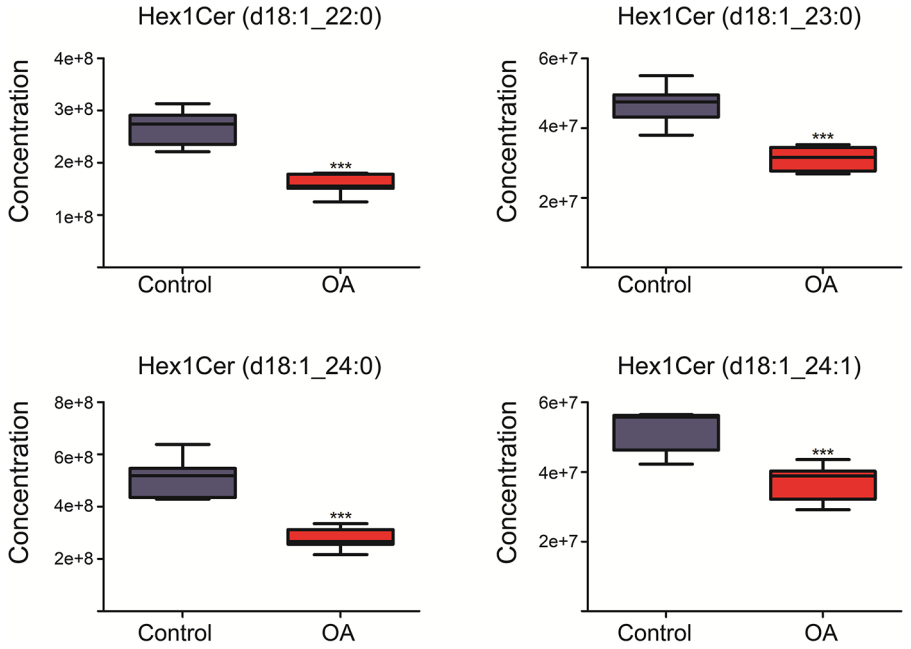

Figure 8. Boxplots of representative hexosylceramide (Hex1Cer) species found significantly decreased in OA-treated groups comparing with control groups. The blue histograms are control groups, and the red histograms are OA-treated groups. T-tests were carried out subsequently. $P < 0.05$ was considered statistically significant. *$P < 0.05$, **$P < 0.01$, ***$P < 0.001$ vs the control.

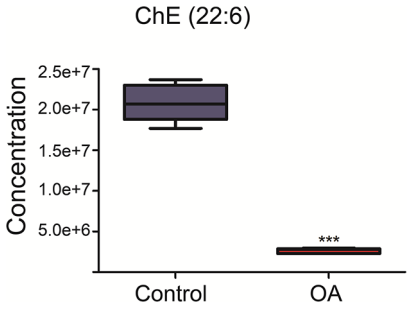

Figure 9. Boxplots of a representative cholesterol ester (ChE) species found significantly decreased in OA-treated groups comparing with control groups. The blue histogram is the control group, and the red histogram is the OA-treated group. A t-test was carried out subsequently. $P < 0.05$ was considered statistically significant. *$P < 0.05$, **$P < 0.01$, ***$P < 0.001$ vs the control.

and cholangiocarcinoma (CCA). Evidence showed that Hex1Cer (d18:1_22:0), Hex1Cer (d18:1_23:0), Hex1Cer (d18:1_24:0), and Hex1Cer (d18:1_24:1) were obviously increased in CHC, NASH, and CCA, and these Hex1Cer's could be the indicator for these liver diseases.[26−28] As the statistical histogram results and the VIP list presented, Hex1Cer was attenuated with OA administration, and Hex1Cer (d18:1_22:0), Hex1Cer (d18:1_23:0), Hex1Cer (d18:1_24:0), and Hex1Cer (d18:1_24:1) were all significantly reduced after OA administration. Similarly, Hex2Cer accumulation was a potential lipid biomarker of alcoholic liver disease,[29] and decreased Hex2Cer was detected in OA-treated groups. The above results indicated that OA administration possessed the property of CLD prevention probable via attenuating the synthesis of Cer, Hex1Cer, and Hex2Cer, and several specific lipids.

DG and TG, components of neutral lipids, were closely associated with liver diseases, particularly TG, as the neutral lipids' core of lipid droplets (LDs) was closely associated with ER homeostasis.[30] The ER was the major site for lipid synthesis in hepatocytes, and ER stress would accelerate NAFLD, while *Schisandra chinensis* extracts possessed a protective property on NAFLD prevention via inhibiting ER stress.[31,32] Furthermore, as reported, TG-rich LDs would ameliorate ER stress as well. Evidence demonstrated that an increased level of TG storage in LDs alleviated tunicamycin-induced ER stress.[33] Similarly, increased TG storage in LDs

https://dx.doi.org/10.1021/acsomega.9b04402
ACS Omega 2020, 5, 11314−11323

could protect human cardiomyocytes from PA-induced ER stress, and OA always was used as a stimulant for TG accumulation.[34] Hence, taken together, OA may provide contributions to ER stress attenuation via increasing the TG storage in LDs, and TG-rich LDs. ChE, another component of neutral lipids, was detected in the liver with NASH.[35] As our results showed, the total content of ChE declined with OA administration, and ChE (22:6), one of ChE with *n*-6 PUFA, was significantly decreased in OA-treated groups. Therefore, ChE could be another lipid metabolite of OA administration for NAFLD prevention, and ChE (22:6) could be a potential biomarker of OA administration on NAFLD prevention.

AcCa and Co as components of fatty acyl compounds were increased and decreased with OA administration, respectively. AcCa possessed neuroprotective properties, especially in Alzheimer's disease (AD) treatment. For example, the levels of AcCa were gradually declined from healthy subjects to subjects with mild cognitive impairment, subjective memory complaint, and up to AD.[36] However, the effects of AcCa on liver disease require further research. Co as the component of acyl-CoA:cholesterol acyltransferase 1 could take part in cholesterol synthesis and stimulate the accumulation of cholesterol, which could promote the progression of liver fibrosis,[37] but more specific knowledge of the effect of Co with OA administration on liver disease prevention is needed.

In addition, there were 478 lipid species detected in the VIP list, which were significantly influenced by OA treatment. These molecules would be potential biomarkers with OA administration. Detailed information about the majority of these compounds on CLD development requires further research.

CONCLUSIONS

An untargeted lipidomics based on HPLC−MS analysis was utilized to investigate changes in endogenous metabolites with OA administration. In total, numerous lipid species influenced by OA treatment were identified, and these identified lipids belonged to 22 lipid classes grouped into four categories. Decreased concentrations of LPC, PG, Cer, Hex1Cer, Hex2Cer, and ChE as well as the increased content of TG were detected with OA administation. Moreover, the 478 lipid species with significant difference after OA treatment could be potential biomarkers of OA administration. Among them, LPC (18:0), PG (16:0_18:1), Cer (d18:1_22:0), Cer (d18:1_24:0), Hex1Cer (d18:1_22:0), Hex1Cer (d18:1_23:0), Hex1Cer (d18:1_24:0), Hex1Cer (d18:1_24:1), and ChE (22:6) were clearly increased in CLD, while these lipid species were significantly decreased after OA treatment. Therefore, this study provided a novel perspective to understand the effects of OA administration on lipid metabolism through investigating endogenous changed lipids via HPLC-MS-based lipidomics.

MATERIALS AND METHODS

Reagents. OA and methanol were purchased from Sigma Aldrich Co. (St. Louis, U.S.A.), and OA was dissolved in dimethylsulfoxide (DMSO) to obtain a stock concentration of 280 mM. Chloroform was obtained from the office of laboratory and equipment management of Nanjing Agricultural University. Methanol and chloroform were of chromatographic grade. Potassium hydroxide (KOH) was purchased from Lingfeng Chemical Reagent. Co. (Shanghai, China).

Cell Culture and Cell Treatments. The human hepatocytes HL-7702 were cultured in RPMI 1640 medium (Hyclone, Logan, USA) containing 10% fetal bovine serum (FBS, Cegrogen, South America) and 1% penicillin−streptomycin solution (Hyclone, Logan, U.S.A.) at 37 °C with 5% CO_2. Hepatocytes at a concentration of 5×10^6 cells/cm^2 were treated with 70 μM OA in DMSO or with the same concentration of DMSO which were termed as control groups. When treated with OA, the 280 mM OA was diluted to 70 mM, and 20 μL of 70 mM OA was added to the growth medium of 20 mL; therefore, the cells were treated with the final concentration of 70 μM OA. In the control groups, 20 μL of DMSO was added to the growth medium for 20 mL. After 12 h, cells were collected for lipid metabolite extraction.

Lipid Metabolite Extraction from Cells. Cells were collected with 1.5 mL of phosphate buffer saline (PBS, Hyclone, Logan, U.S.A.) and transferred to a glass tube. The cells were mixed with four volumes of the organic phase made up with chloroform and methanol at a volume ratio of 2:1. Subsequently, the mixture was adequately vibrated several times and centrifuged at 3000 rpm for 15 min. After that, the mixture was separated in three parts: the top layer was the aqueous phase, the middle layer was the protein phase, and the lower layer was the organic phase. The lower organic layer was collected by a glass syringe to a new glass tube, avoiding picking any protein up, and then dried by a nitrogen gas. The dried lipid extract was stored at −80 °C until further analysis. At last, the protein phase was dissolved with 0.1 M KOH at 4 °C overnight, and the protein concentration was determined using the BCA protein quantitation kit (Beyotime, Shanghai, China). The redissolution volume of dried lipid metabolite extraction was normalized based on the protein concentration. The method of lipid metabolite extraction was carried out according to the protocol provided by Tsinghua University.[38]

HPLC Methods for Lipid Metabolites. Orbitrap QEHF coupled with Ultimate 3000 HPLC (Thermo, CA) was used for lipidomics analysis. Lipid extracts were analyzed by HPLC using a Cortecs C18 column (2.1 × 100 mm, Waters) both in positive and negative modes. The elution solvent system contained a mix of mobile phase A (acetonitrile (ACN):H_2O (60:40), 10 mM ammonium acetate) and mobile phase B (isopropanol:ACN (90:10), 10 mM ammonium acetate), which were utilized both in positive and negative modes. The detailed elution gradient was as follows: 0 min, 37% B; 1.5 min, 37% B; 4 min, 45% B; 5 min, 52% B; 8 min, 58% B; 11 min, 66% B; 14 min,70% B; 18 min, 75% B; 20 min, 98% B; 22 min, 98% B; 22.1 min 37%B; and 25 min, 37% B. The dried lipid metabolite extraction preparations were redissolved, and the redissolutions of OA treated and control samples were injected into the column randomly for analysis, following the parameter setting above. The QC samples, consisting of a mixture of OA-treated samples and control samples, were inserted before or after OA-treated samples and control samples. They were used to evaluate the stability of the instrument in order to provide repeatable and high-quality data. The data of QC samples are in the original data and may be downloaded from the website for reference. In the analysis, PC (14:0_14:0) was added in the samples as internal standards at a concentration of 2 μg/mL. The method was carried out essentially as in the protocol provided by Tsinghua University.[38]

MS Methods for Lipid Metabolites. A Q Exactive Orbitrap mass spectrometer (Thermo, CA) was used for lipid

https://dx.doi.org/10.1021/acsomega.9b04402
ACS Omega 2020, 5, 11314−11323

metabolites analysis. Mass range (m/z) was set as 240−2000 for the positive mode and 200−2000 for negative mode. The spray voltage was different between positive mode and negative mode, which was 3.2 and 2.8 kV, respectively. The capillary temperature was kept at 320 °C for all analyses. Furthermore, the remaining parameters were as follows: sheath gas flow rate (arb), 35; aux gas flow rate (arb), 10; topN, 10; NCE, 15/30/45; and duty cycle, 1.2 s. The method of MS analysis was performed according to the protocol provided by Tsinghua University.[38]

Data Analysis. Lipids were identified according to matching precursor and characteristic fragment masses. A 5 ppm and 10 ppm mass tolerance was used for precursors and fragments, respectively. A 0.25 min retention time shift was allowed for quantitation.[38] For statistical analysis, PCA, an unsupervised pattern recognition model, and OPLS-DA, a supervised pattern recognition model, were utilized to construct the predictive models to assess the difference between OA-treated groups and control groups. The VIP list (VIP > 1.0 and $P < 0.05$) obtained from OPLS-DA was used to determine significantly changed metabolites after OA treatment. Volcano plots and heat maps were generated using MetaboAnalyst 3.0, an online data analysis system. These statistics compensate for analyzing many metabolites at the same time and were based on the conversion from the p value to FDR (p value) (https://www.metaboanalyst.ca/faces/ModuleView.xhtml). A t-test was used for comparing the differences between OA-treated groups and control groups. There were seven biological parallels for both OA-treated and control groups, and the significance level was set at $P < 0.05$.

AUTHOR INFORMATION

Corresponding Author

Rong Liu − *College of Food Science and Technology, Nanjing Agricultural University, Nanjing 210095, China; National Center for International Research on Animal Gut Nutrition, Nanjing 210095, China; Jiangsu Collaborative Innovation Center of Meat Production and Processing, Nanjing 210095, China;* orcid.org/0000-0002-1996-0015; Email: liurong010@njau.edu.cn

Authors

Chao Xu − *College of Food Science and Technology, Nanjing Agricultural University, Nanjing 210095, China*

Dan Song − *College of Food Science and Technology, Nanjing Agricultural University, Nanjing 210095, China*

Askild L. Holck − *NOFIMA - Norwegian Institute of Food, Fisheries and Aquaculture Research, N-1431 Aas, Norway*

Youyou Zhou − *College of Food Science and Technology, Nanjing Agricultural University, Nanjing 210095, China*

Complete contact information is available at: https://pubs.acs.org/10.1021/acsomega.9b04402

Notes

The authors declare no competing financial interest.

ACKNOWLEDGMENTS

The work was supported by grants to R.L. from the National Key Research and Development Program of China (grant no.2017YFD0400200), Jiangsu Natural Science Funds for Distinguished Young Scholar (grant no. BK20170025), National Natural Science Foundation of China (grant no. 31771532), and "Shuangchuang", "Six Talent Peaks", and "333" projects in Jiangsu province. We also appreciate the support from the Metabolomics Center of Tsinghua University, National Protein Science Facility for the technology support during acquisition and data analysis of lipidomic profiles.

REFERENCES

(1) Katdare, A.; Thakkar, S.; Dhepale, S.; Khunt, D.; Misra, M. Fatty acids as essential adjuvants to treat various ailments and their role in drug delivery: A review. *Nutrition* **2019**, *65*, 138−157.

(2) Soto-Alarcon, S. A.; Valenzuela, R.; Valenzuela, A.; Videla, L. A. Liver Protective Effects of Extra Virgin Olive Oil: Interaction between Its Chemical Composition and the Cell-signaling Pathways Involved in Protection. *EMIDDT* **2018**, *18*, 75−84.

(3) Embade, N.; Millet, O. Molecular Determinants of Chronic Liver Disease as Studied by NMR-Metabolomics. *Curr. Top. Med. Chem.* **2017**, *17*, 2752−2766.

(4) Messner, D. J.; Kowdley, K. V. Biting the iron bullet: endoplasmic reticulum stress adds the pain of hepcidin to chronic liver disease. *Hepatology* **2010**, *51*, 705−707.

(5) Ratziu, V.; Poynard, T. Assessing the outcome of nonalcoholic steatohepatitis? It's time to get serious. *Hepatology* **2006**, *44*, 802−805.

(6) Hirata, T.; Kawai, T.; Hirose, H.; Tanaka, K.; Kurosawa, H.; Fujii, C.; Fujita, H.; Seto, Y.; Matsumoto, H.; Itoh, H. Palmitic acid-rich diet suppresses glucose-stimulated insulin secretion (GSIS) and induces endoplasmic reticulum (ER) stress in pancreatic islets in mice. *Endocr. Res.* **2016**, *41*, 8−15.

(7) Martínez, L.; Torres, S.; Baulies, A.; Alarcón-Vila, C.; Elena, M.; Fabriás, G.; Casas, J.; Caballeria, J.; Fernandez-Checa, J. C.; García-Ruiz, C. Myristic acid potentiates palmitic acid-induced lipotoxicity and steatohepatitis associated with lipodystrophy by sustaning de novo ceramide synthesis. *Oncotarget* **2015**, *6*, 41479−41496.

(8) Pardo, V.; González-Rodríguez, Á.; Muntané, J.; Kozma, S. C.; Valverde, Á. M. Role of hepatocyte S6K1 in palmitic acid-induced endoplasmic reticulum stress, lipotoxicity, insulin resistance and in oleic acid-induced protection. *Food Chem. Toxicol.* **2015**, *80*, 298−309.

(9) Chen, X.; Li, L.; Liu, X.; Luo, R.; Liao, G.; Li, L.; Liu, J.; Cheng, J.; Lu, Y.; Chen, Y. Oleic acid protects saturated fatty acid mediated lipotoxicity in hepatocytes and rat of non-alcoholic steatohepatitis. *Life Sci.* **2018**, *203*, 291−304.

(10) Lee, J. Y.; Moon, J. H.; Park, J. S.; Lee, B. W.; Kang, E. S.; Ahn, C. W.; Lee, H. C.; Cha, B. S. Dietary oleate has beneficial effects on every step of non-alcoholic Fatty liver disease progression in a methionine- and choline-deficient diet-fed animal model. *Diabetes Metab J* **2011**, *35*, 489−496.

(11) Malhi, H.; Gores, G. J. Molecular mechanisms of lipotoxicity in nonalcoholic fatty liver disease. *Seminars in liver disease* **2008**, *28*, 360−369.

(12) Homan, R.; Grossman, J. E.; Pownall, H. J. Differential effects of eicosapentaenoic acid and oleic acid on lipid synthesis and secretion by HepG2 cells. *J. Lipid Res.* **1991**, *32*, 231−241.

(13) Han, X.; Gross, R. W. Global analyses of cellular lipidomes directly from crude extracts of biological samples by ESI mass spectrometry: a bridge to lipidomics. *J. Lipid Res.* **2003**, *44*, 1071−1079.

(14) Yang, L.; Li, M.; Shan, Y.; Shen, S.; Bai, Y.; Liu, H. Recent advances in lipidomics for disease research. *J. Sep. Sci.* **2016**, *39*, 38−50.

(15) Whelehan, O. P.; Earll, M. E.; Johansson, E.; Toft, M.; Eriksson, L. Detection of ovarian cancer using chemometric analysis of proteomic profiles. *Chemometr Intell Lab Syst.* **2006**, *84*, 82−87.

(16) Zhou, L.-F.; Zhao, B.-W.; Guan, N.-N.; Wang, W.-M.; Gao, Z.-X. Plasma metabolomics profiling for fish maturation in blunt snout bream. *Metabolomics* **2017**, *13*, 40.

(17) Wang, J.; Li, Z.; Chen, J.; Zhao, H.; Luo, L.; Chen, C.; Xu, X.; Zhang, W.; Gao, K.; Li, B.; Zhang, J.; Wang, W. Metabolomic

identification of diagnostic plasma biomarkers in humans with chronic heart failure. *Mol. BioSyst.* **2013**, *9*, 2618−2626.
(18) Shannon, W.; Culverhouse, R.; Duncan, J. Analyzing microarray data using cluster analysis. *Pharmacogenomics* **2003**, *4*, 41−52.
(19) Han, M. S.; Park, S. Y.; Shinzawa, K.; Kim, S.; Chung, K. W.; Lee, J. H.; Kwon, C. H.; Lee, K. W.; Lee, J. H.; Park, C. K.; Chung, W. J.; Hwang, J. S.; Yan, J. J.; Song, D. K.; Tsujimoto, Y.; Lee, M. S. Lysophosphatidylcholine as a death effector in the lipoapoptosis of hepatocytes. *J. Lipid Res.* **2007**, *49*, 84−97.
(20) Gorden, D. L.; Myers, D. S.; Ivanova, P. T.; Fahy, E.; Maurya, M. R.; Gupta, S.; Min, J.; Spann, N. J.; McDonald, J. G.; Kelly, S. L.; Duan, J.; Sullards, M. C.; Leiker, T. J.; Barkley, R. M.; Quehenberger, O.; Armando, A. M.; Milne, S. B.; Mathews, T. P.; Armstrong, M. D.; Li, C.; Melvin, W. V.; Clements, R. H.; Washington, M. K.; Mendonsa, A. M.; Witztum, J. L.; Guan, Z.; Glass, C. K.; Murphy, R. C.; Dennis, E. A.; Merrill, A. H., Jr.; Russell, D. W.; Subramaniam, S.; Brown, H. A. Biomarkers of NAFLD progression: a lipidomics approach to an epidemic. *J. Lipid Res.* **2015**, *56*, 722−736.
(21) Chang, X.; Wang, Z.; Zhang, J.; Yan, H.; Bian, H.; Xia, M.; Lin, H.; Jiang, J.; Gao, X. Lipid profiling of the therapeutic effects of berberine in patients with nonalcoholic fatty liver disease. *J Transl Med* **2016**, *14*, 266.
(22) Sanyal, A. J.; Pacana, T. A Lipidomic Readout of Disease Progression in A Diet-Induced Mouse Model of Nonalcoholic Fatty Liver Disease. *Trans. Am. Clin. Climatol. Assoc.* **2015**, *126*, 271−288.
(23) Kasumov, T.; Li, L.; Li, M.; Gulshan, K.; Kirwan, J. P.; Liu, X.; Previs, S.; Willard, B.; Smith, J. D.; McCullough, A. Ceramide as a mediator of non-alcoholic Fatty liver disease and associated atherosclerosis. *PLoS One* **2015**, *10*, No. e0126910.
(24) Kurek, K.; Piotrowska, D. M.; Wiesiołek-Kurek, P.; Łukaszuk, B.; Chabowski, A.; Górski, J.; Żendzian-Piotrowska, M. Inhibition of ceramide de novo synthesis reduces liver lipid accumulation in rats with nonalcoholic fatty liver disease. *Liver Int* **2014**, *34*, 1074−1083.
(25) Wasilewska, N.; Bobrus-Chociej, A.; Harasim-Symbor, E.; Tarasów, E.; Wojtkowska, M.; Chabowski, A.; Lebensztejn, D. M. Increased serum concentration of ceramides in obese children with nonalcoholic fatty liver disease. *Lipids Health Dis.* **2018**, *17*, 216.
(26) Li, J. F.; Qu, F.; Zheng, S. J.; Ren, J. Y.; Wu, H. L.; Liu, M.; Liu, H.; Ren, F.; Chen, Y.; Zhang, J. L.; Duan, Z. P. Plasma Sphingolipids as Potential Indicators of Hepatic Necroinflammation in Patients with Chronic Hepatitis C and Normal Alanine Aminotransferase Level. *PLoS One* **2014**, *9*, e95095.
(27) Apostolopoulou, M.; Gordillo, R.; Koliaki, C.; Gancheva, S.; Jelenik, T.; De Filippo, E.; Herder, C.; Markgraf, D.; Jankowiak, F.; Esposito, I.; Schlensak, M.; Scherer, P. E.; Roden, M. Specific Hepatic Sphingolipids Relate to Insulin Resistance, Oxidative Stress, and Inflammation in Nonalcoholic Steatohepatitis. *Diabetes Care* **2018**, *41*, 1235−1243.
(28) Silsirivanit, A.; Phoomak, C.; Teeravirote, K.; Wattanavises, S.; Seubwai, W.; Saengboonmee, C.; Zhan, Z.; Inokuchi, J.-i.; Suzuki, A.; Wongkham, S. Overexpression of HexCer and LacCer containing 2-hydroxylated fatty acids in cholangiocarcinoma and the association of the increase of LacCer (d18:1-h23:0) with shorter survival of the patients. *Glycoconj. J.* **2019**, *36*, 103−111.
(29) Meikle, P. J.; Mundra, P. A.; Wong, G.; Rahman, K.; Huynh, K.; Barlow, C. K.; Duly, A. M. P.; Haber, P. S.; Whitfield, J. B.; Seth, D. Circulating Lipids Are Associated with Alcoholic Liver Cirrhosis and Represent Potential Biomarkers for Risk Assessment. *PLoS One* **2015**, *10*, No. e0130346.
(30) Welte, M. A.; Gould, A. P. Lipid droplet functions beyond energy storage. *Biochim. Biophys. Acta, Mol. Cell Biol. Lipids* **2017**, *1862*, 1260−1272.
(31) Lee, J. S.; Zheng, Z.; Mendez, R.; Ha, S. W.; Xie, Y.; Zhang, K. Pharmacologic ER stress induces non-alcoholic steatohepatitis in an animal model. *Toxicol. Lett.* **2012**, *211*, 29−38.
(32) Jang, M. K.; Nam, J. S.; Kim, J. H.; Yun, Y. R.; Han, C. W.; Kim, B. J.; Jeong, H. S.; Ha, K. T.; Jung, M. H. Schisandra chinensis extract ameliorates nonalcoholic fatty liver via inhibition of endoplasmic reticulum stress. *J. Ethnopharmacol.* **2016**, *185*, 96−104.
(33) Fuchs, C. D.; Claudel, T.; Kumari, P.; Haemmerle, G.; Pollheimer, M. J.; Stojakovic, T.; Scharnagl, H.; Halilbasic, E.; Gumhold, J.; Silbert, D.; Koefeler, H.; Trauner, M. Absence of adipose triglyceride lipase protects from hepatic endoplasmic reticulum stress in mice. *Hepatology* **2012**, *56*, 270−280.
(34) Bosma, M.; Dapito, D. H.; Drosatos-Tampakaki, Z.; Huiping-Son, N.; Huang, L. S.; Kersten, S.; Drosatos, K.; Goldberg, I. J. Sequestration of fatty acids in triglycerides prevents endoplasmic reticulum stress in an in vitro model of cardiomyocyte lipotoxicity. *Biochim. Biophys. Acta* **2014**, *1841*, 1648−1655.
(35) Puri, P.; Baillie, R. A.; Wiest, M. M.; Mirshahi, F.; Choudhury, J.; Cheung, O.; Sargeant, C.; Contos, M. J.; Sanyal, A. J. A lipidomic analysis of nonalcoholic fatty liver disease. *Hepatology* **2007**, *46*, 1081−1090.
(36) Cristofano, A.; Sapere, N.; La Marca, G.; Angiolillo, A.; Vitale, M.; Corbi, G.; Scapagnini, G.; Intrieri, M.; Russo, C.; Corso, G.; Di Costanzo, A. Serum Levels of Acyl-Carnitines along the Continuum from Normal to Alzheimer's Dementia. *PLoS One* **2016**, *11*, No. e0155694.
(37) Tomita, K.; Teratani, T.; Suzuki, T.; Shimizu, M.; Sato, H.; Narimatsu, K.; Usui, S.; Furuhashi, H.; Kimura, A.; Nishiyama, K.; Maejima, T.; Okada, Y.; Kurihara, C.; Shimamura, K.; Ebinuma, H.; Saito, H.; Yokoyama, H.; Watanabe, C.; Komoto, S.; Nagao, S.; Sugiyama, K.; Aosasa, S.; Hatsuse, K.; Yamamoto, J.; Hibi, T.; Miura, S.; Hokari, R.; Kanai, T. Acyl-CoA:cholesterol acyltransferase 1 mediates liver fibrosis by regulating free cholesterol accumulation in hepatic stellate cells. *J. hepatol.* **2014**, *61*, 98−106.
(38) Tang, H.; Wang, X.; Xu, L.; Ran, X.; Li, X.; Chen, L.; Zhao, X.; Deng, H.; Liu, X. Establishment of local searching methods for orbitrap-based high throughput metabolomics analysis. *Talanta* **2016**, *156-157*, 163−171.

https://dx.doi.org/10.1021/acsomega.9b04402
ACS Omega 2020, 5, 11314−11323